Blimp-Borne Laser Communication Technology Based on Space Dynamic Base Station

Tong Wang, Xin Zhao, Chao Lv, Junyao Wang, Yansong Song, Xiaonan Yu, Chang Zhou, and Ning An

***Abstract*—Space dynamic communication base stations are characterized by high mobility, flexible deployment and wide coverage. It has a wide range of needs in the fields of emergency communication, earthquake relief and island communication. To solve the problem of a limited number of users due to the limited bandwidth of space base stations, so we should improve the reliability and efficiency of data transmission between space mobile base stations. According to the characteristics of the airship platform, a blimp-borne laser communication terminal applied to space dynamic base stations is designed to meet the demand for bi-directional transmission of 5G signal laser carriers in space between airships. The experimental results show that the blimp-borne laser communication terminal achieves an overall technical index of capture probability is better than 98%, the average capture time is 5s, the tracking accuracy is better than 6–15 μrad, the communication rate is 2.5 Gbps and BER is 1E-7. In order to realize the real-time evaluation of the performance of laser communication system under the turbulent channel and guide the research of anti-turbulence fading method, a real-time test method of communication channel turbulence characteristics based on the principle of light intensity scintillation is proposed. And the real-time test of turbulence characteristics of airship inclined link and the horizontal link is completed. The research results play a positive role in promoting the development of 5G mobile technology and space optical communication technology.**

***Index Terms*—5G dynamic base station, free space optical communication, blimp-borne laser communication, turbulence characteristics.**

I. Introduction

With the development of mobile network information age, the fifth generation (5G) network is gradually becoming the pathway for high-speed information interaction in areas such as large-scale Internet of Things, industrial automation and unmanned vehicles. However, the construction of 5G base stations are limited by issues such as area, population density and cost, for this reason, remote mountain villages and islands are still without wireless network coverage. The establishment of space base stations (SBS) effectively solve the demand for wireless communication networks with high cost, small number of users and wide coverage. Dynamic platforms such as airships, aircraft and satellites are equipped with wireless base stations to constitute SBS, which can achieve efficient signal coverage with their unique communication line-of-sight links [1]. The U.S. company SpaceX proposed the "Musk Starlink Project" in 2015, which plans to achieve high-speed communication through 12000 low-orbiting satellites. The Starlink does not rely on ground-based base stations and is able to provide broadband services to suburban areas, agricultural areas and other areas through the advantage of large satellite coverage. However, the communication rate is currently only 300Mbps due to the speed of data transmission between satellites.

Facing the demand for high-capacity data transmission between satellites and between base stations, free-space optical communication (FSOC) technology is the best way to solve the high-speed transmission of backbone data between satellites, base stations, and nodes [2] by virtue of fast chain building speed [3], high transmission rate [4], good confidentiality performance [5], and strong anti-interference capability [6]. At present, space laser communication is widely used in airships, aircraft, satellites and other fields. In 2017, Bruce Moision *et al.* proposed the Loon project [7], which used a high-altitude balloon to build a FSOC experiment in the stratosphere at an altitude of 20 km, achieving a link distance of 100 km and a communication rate of 130 Mbps full-duplex data transmission. In 2017 Yu Siyuan et al, simulated a communication link between a satellite and the ground and built a FSOC experiment [8] with a link distance of 11.16 km under weak turbulence conditions, achieving a data transmission at a communication rate of 300 Mbps. In 2019, Li Long *et al.* built a laser communication experiment between ground stations over a round-trip distance of 100 m via an unmanned UAV and used MIMO equalization techniques to mitigate turbulence effects to achieve dual-channel 20 Gbps data transmission [9]. In 2020, Yu Xiaonan *et al.* conducted FSOC experiments between airships to the ground and transmitted 5G network data via a laser communication link [10]. A laser link communication rate of 2.5 Gbps and a 5G network terminal download rate of 854 Mbps were achieved at a 1 km link distance.

Manuscript received June 30, 2021; revised July 25, 2021; accepted August 4, 2021. Date of publication August 12, 2021; date of current version September 21, 2021. This work was supported in part by the Project of Jilin Provincial Development and Reform Commission "Ultra precision positioning fast mirror system" (2020C023-1), in part by the National Natural Science Youth Foundation of China under Grant 61701045, and in part by the Science and Technology Development Plan of Jilin Province (2020081050GH). *(Corresponding author: Xin Zhao.)*

Tong Wang, Xin Zhao, and Chao Lv are with the School of Electric and Information Engineering, Changchun University of Science and Technology, Changchun 130022, China (e-mail: wxt021244@163.com; gps.ins@163.com; lvchao@cust.edu.cn).

Junyao Wang, Yansong Song, Xiaonan Yu, and Chang Zhou are with the Key Laboratory of Photoelectric Measurement and Control and Optical Information Transfer Technology of Ministry of Education, Changchun University of Science and Technology, Changchun 130022, China (e-mail: 2020200055@mails.cust.edu.cn; 2009800048@cust.edu.cn; yuxiaonan@cust.edu.cn; 2019100154@mails.cust.edu.cn).

Ning An is with the Changchun Observatory, National Astronomical Observatories, Chinese Academy of Sciences, Changchun 130117, China (e-mail: ann@cho.ac.cn).

Digital Object Identifier 10.1109/JPHOT.2021.3103426

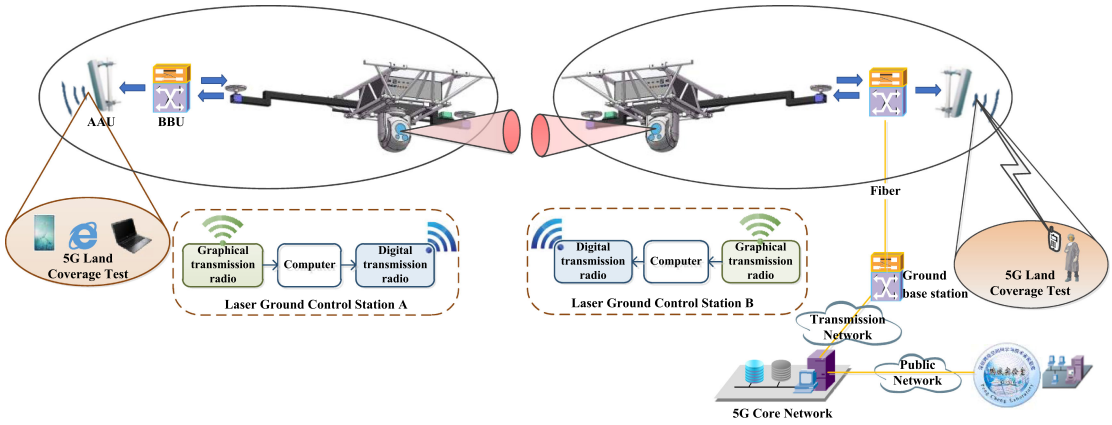

Fig. 1. Composition and working principle of FSOC based blimp-borne dynamic base station.

During the development of FSOC systems in airships, aircraft, and satellites, the laser communication links are highly susceptible to the atmospheric channel environment, which causes energy fading, random changes in amplitude and phase, and beam drift. These effects limit the performance parameters such as rate and BER of the FSOC system. Three adaptive modulation and adaptive coding schemes with radio frequency (RF) feedback [11] were proposed by Djordjevic *et al.* The results show that a simple channel inversion scheme performs comparable to a variable-rate variable-power adaptation scheme in the weak turbulence regime. Under strong turbulence conditions, a variable variable-rate variable-power scheme or truncated channel inversion is required to mitigate the impact of strong turbulence on the communication. The article also describes the adaptive LDPC-coded modulation scheme, which enables communication in the power saturation regime is possible. A channel-aware blind bit-rate adaptation technique [12] was proposed by Guiomar F.P. *et al.* They combined the proposed channel estimation technique with highly flexible modulation enabled by time-adaptive probabilistic constellation shaping (PCS), enabling 400G+ transmission over 55 m during unstable atmospheric conditions.

For the demand of high-capacity data transmission between SBS, this paper designs a blimp-borne laser communication system (BLCS) applicable to SBS, and introduces the system composition and working principle. In response to the needs of airship platform motion characteristics and 5G network data transmission characteristics, the GPS/INS combination of dynamic pointing and capturing, coarse and precise composite axis tracking, and avalanche photodiode (APD) gain automatic control technologies are designed. In order to realize the performance evaluation of BLCS under atmospheric turbulence channel and the research of anti-atmospheric turbulence fading method, the real-time measurement method of atmospheric turbulence of communication channel based on the principle of light intensity scintillation is proposed, and the real-time measurement of turbulence characteristics of inclined link and the horizontal link is carried out. We also built 5G network transmission experiments under the space-space laser communication link, which provided technical support for the application of a space laser communication system in 5G networks and SBS.

II. System Composition Principle

The space dynamic base station requires the realization of high-speed transmission of 5G signals between the airship-airship dual dynamic base station and the airship-ground stationary base station through the space laser terminal, which is connected to the city 5G core network after the airship laser communication terminal is connected to the blimp-borne Building Baseband Unit (BBU) through an optical fiber. At the same time, the airship is mounted with an Active Antenna Unit (AAU) to provide 5G network services for users. The basic composition and working principle of the system are shown in Fig. 1.

Based on the above principle, it is possible to establish high-speed data interaction between SBS through a blimp-borne space laser communication system. The antenna of the 5G network carried by the blimp achieves a wide range of wireless network coverage, and the maximum coverage radius can reach 20 km, which meets the demand for rapid recovery and application of 5G network in an emergency, earthquake mitigation, remote areas and other regions. The blimp-borne laser communication terminal can also be connected to low-orbiting satellites, UAVs and other equipment that can carry laser communication systems to build an efficient and reliable information transmission network.

For the above-mentioned application requirements, the blimp-borne laser communication terminal is designed. The system consists of five main parts: optical and mechanical subsystem, PAT (pointing, capturing, tracking) subsystem, communication transceiver subsystem, 5G and laser transmission baseband signal conversion subsystem, and general control subsystem. Among them, the communication laser wavelength is 1550/1530 nm band and the beacon laser is 785/830nm band. The optical antenna is Cassegrain structure with transceiver common aperture structure, PAT subsystem is

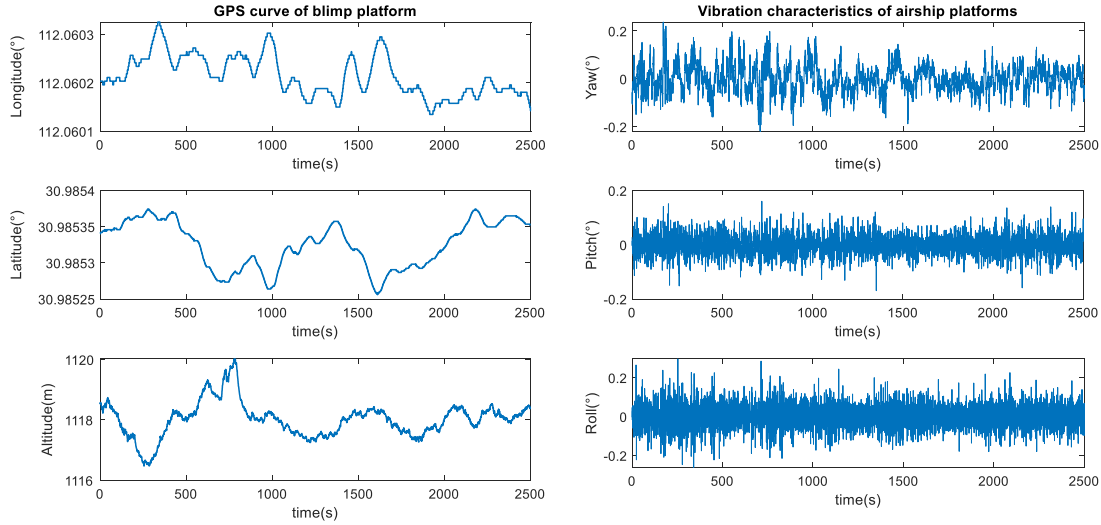

Fig. 2. Vibration characteristics test results of blimp platform.

TABLE I
THE MAIN PARAMETERS OF BLCS DESIGN

Parameters	Indicators	
Laser wavelength	Beacon	785/830nm
	Communication	1550/1530nm
Divergence angle	Beacon	2mrad
	Communication	100μrad
Optical Aperture		100mm
Communication rate		1.25/2.5Gbps
Tracking accuracy		5μrad
Receiving field of view		60mrad

coarse and fine composite axis structure, and the communication mode is intensity modulation/direct detection (IM/DD). The basic parameters of the system design are shown in Table I.

III. PAT SUBSYSTEM DESIGN AND EXPERIMENTAL TESTING

A. Blimp Platform Movement Characteristics

High probability and fast capture with high dynamic and high accuracy tracking are the key core technologies of the PAT system [13], which are the prerequisite and guarantee for proper communication. In order to reduce the size of the uncertainty area captured by the BLCS, a combined dual-antenna GPS/INS navigation system is incorporated into the system design to provide position, latitude, and time parameters for the blimp terminal. At the same time, based on the combined navigation system to complete the test of the airborne motion characteristics of the blimp platform. The test conditions were: average longitude 112.0602°, average latitude 30.9853° and average altitude 1118.0 m after the blimp lifted off. Its typical vibration characteristics in the air are shown in Fig. 2.

After several measurements, the maximum motion speed of the blimp platform in the yaw was 0.2372°/s, the maximum motion speed in pitch was 0.1693°/s, and the maximum motion speed in cross roll was 0.2966°/s. The above platform motion characteristics are an important reference and basis for PAT system design.

B. Pointing and Capturing Unit

Based on the characteristics of the blimp platform, GPS/INS is used to provide position and latitude information, and the initial pointing modeling of the visual axis is based on the coordinate matrix principle. The model equation is as follows [14]:

$$[x\ y\ z]^T = C_b^r C_n^b C_e^n [X_1 - X\ Y_1 - Y_2\ Z_1 - Z_2]^T \quad (1)$$

$$\alpha = \arctan(x/y); \beta = \arctan\left(z \Big/ \sqrt{x^2 + y^2}\right) \quad (2)$$

where, α is the azimuthal angle of rotation of the view axis, in degrees. β is the pitch angle of view axis rotation, in degrees. (x, y, z) is the coordinate value of the view axis, (X1, Y1, Z1) is the coordinate value in the local WGS-84 coordinate system, (X2, Y2, Z2) is the coordinate value in the target WGS-84 coordinate system. C_b^r is the conversion matrix from WGS-84 coordinate system to ENU coordinate system, C_n^b is the conversion matrix from ENU coordinate system to carrier coordinate system, and C_e^n is the conversion matrix from carrier coordinate system to optical transmitter installation coordinate system.

The positioning error of the selected GPS system is 10 m, when the distance is 12 km, the error is $\sigma_1 = 1.44$ mrad. The latitude measurement error is $\sigma_2 = 2.43$ mrad, the turntable pointing error is $\sigma_3 = 50$ μrad, the platform stability error is $\sigma_4 = 0.35$ mrad, and the error of dynamic hysteresis is $\sigma_5 = 7.26$ μrad. The final pointing error is:

$$\sigma = \sqrt{\sigma_1^2 + \sigma_2^2 + \sigma_3^2 + \sigma_4^2 + \sigma_5^2} = 2.85 \text{ mrad} \quad (3)$$

In order to meet the full coverage of the blimp-borne optical terminal, the uncertainty area is required to be more than three

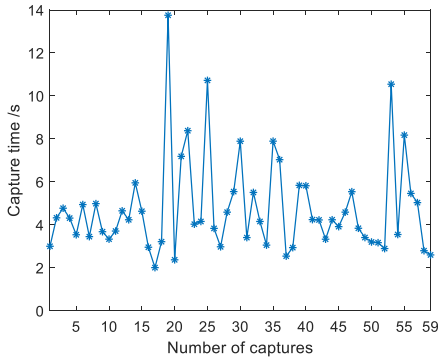

Fig. 3. Capture time test results.

times of the pointing error, therefore, the uncertainty area size of the system is set at 10 mrad.

Since the received field-of-view angle can completely cover the uncertain region at design time, the beacon capture is achieved by gaze-scan mode, and the scan mode is spiral scan, and the spiral scan trajectory in polar coordinates [15] is

$$r_p = \frac{d}{2\pi}\theta_p \tag{4}$$

where d is the pitch and (r_p, θ_p) is a point in the spiral scanning polar coordinates. The corresponding capture time is

$$T_0 = \left[\frac{\theta_{unc}^2}{\theta_{fov}^2 \times \varepsilon}\right] \times T_1 \times N \tag{5}$$

where θ_{unc} is the uncertainty area size; θ_{fov} is the received field of view angle; T_1 is the dwell time; N is the number of scanned areas at the transmitter side (this system N= 1); $\varepsilon = (1-k)^2$ and k are the overlap factors.

Based on the above principle, the capture test of the laser communication terminal between the two blimps was completed. The experimental results are shown in Fig. 3 . During the experiment a total of 60 capture experiments were performed. There were 59 successful captures in these experiments, with a capture probability of over 98%. The average capture time was 4.97s.

C. Composite Axis Tracking Technology

The blimp-borne terminal adopts coarse and fine composite axis tracking structure. The system guides the beacon beam spot into the coarse tracking field of view through open-loop pointing and scanning, and after realizing the coarse tracking system optical closed-loop control, the off-target amount of the beam spot is smaller than the fine tracking field of view. And enter the fine tracking field of view, finally forming a coarse and fine two-stage optical closed-loop control. The tracking accuracy of the compound axis system is determined by the fine tracking system. The blimp-borne terminal system is designed with a tracking accuracy of 5 μrad, mainly considering the beam spot detection error, dynamic hysteresis error, and platform vibration residuals on the fine tracking system. When operating in the atmospheric channel, the blimp-borne terminal is inevitably

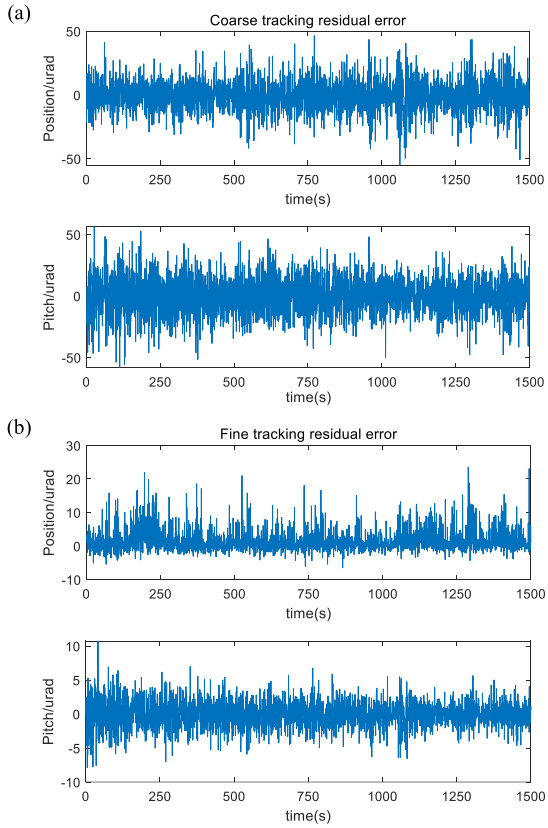

Fig. 4. 12km air-to-air laser communication test tracking accuracy curve (a) Coarse tracking residuals (b) Composite tracking accuracy (fine tracking residuals).

affected by atmospheric turbulence. The light intensity scintillation effect in atmospheric turbulence directly leads to the increase of communication error rate and interruption rate, and the light spot expansion effect in turbulence directly leads to the decrease of light spot detection accuracy, which in turn makes the system tracking accuracy lower than the design value. The tracking accuracy of the composite axis system is tested in the turbulence channel during the experiment. The following figure gives the results of one test.

The above results show that turbulence has no effect on the coarse tracking system because, the residuals of the coarse tracking system are greater than the effect of turbulence. However, turbulence has a large impact on the fine tracking system, and the tracking accuracy has reached 10 μrad, which is much larger than the design value. The above results are for a moderately weak turbulence $C_N^2 = 1.4 \times 10^{-16} m^{-2/3}$ (see Eqs. 7-8 for the specific test principle). The tracking accuracy of this system under moderate to weak turbulence is shown to be between 6 and 15 μrad by several measurements. In order to reduce the alignment or tracking power loss, the tracking accuracy of the PAT system is required to be between 1/6–1/8 of the communication beam scatter angle. The communication beam scatter angle of this system is 100 μrad, and the tracking accuracy is designed to be 6–15 μrad, which basically meets the design tracking requirements.

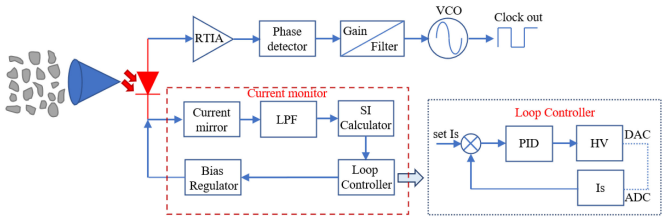

Fig. 5. APD gain automatic control method system block diagram.

IV. Communication Subsystem Design and Testing

The 5G core network data transmission uses HTTP/2 protocol with peak rates up to 10 Gbps, while requiring communication BER better than 1E-6 orders of magnitude. The 5G signal needs to be converted to a baseband signal for network data reorganization before laser carrier transmission. 8B/10B coding is used to avoid the phenomenon of "1" and "0" in data transmission. Therefore, the design of a laser communication system should meet the data transmission requirements of 2.5 Gbps communication rate, 1E-7 communication bit error rate and full duplex communication method.

The design laser communication mode is Intensity Modulation/Direct Detection (IM/DD), where the encoded baseband signal is loaded on the laser by OOK modulation, amplified by an optical amplifier and shaped by an optical antenna to achieve 2.5 Gbps optical signal transmission.

High-rate optical signals transmitted in atmospheric channels are highly susceptible to the effects of atmospheric turbulence. The scintillation effect in turbulence [16] causes the far-field beam to exhibit strong fluctuations in the time and space domains, causing fluctuations in the received optical intensity and leading to an increase in the BER of the communication system [17]. To ensure that the link BER meets the 5G signal transmission requirements, the APD gain factor automatic control technique is designed at the communication receiver side, as shown in Fig. 5.

The APD gain factor automatic control technique is based on the real-time evaluation of the laser communication system under turbulent channels. By the characteristic of APD gain factor MAPD changes with APD bias voltage VAPD, the conversion equation is as follows.

$$M_{APD} \approx (5.87E-9)\exp(0.29V_{APD}) \tag{6}$$

The gain factor is changed with the strength of atmospheric turbulence to stabilize the APD output signal and improve the received signal-to-noise ratio. The speed of turbulent channel evaluation in the automatic control process determines the speed of APD adaptive control follow-up, for which a real-time measurement method of channel turbulence characteristics is proposed. The APD photogenerated current signal is extracted by a current mirror at the communication receiver, and the channel turbulence characteristics are obtained in real-time without affecting the communication according to the light intensity

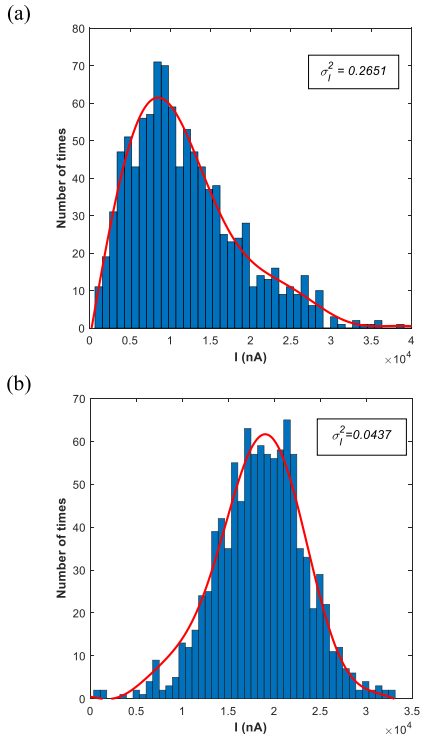

Fig. 6. Scintillation variance energy distribution for control and uncontrolled conditions (a) Uncontrolled; (b) Automatic control.

scintillation intensity calculation formula. The scintillation index (SI) is calculated by the formula.

$$\sigma_I^2 = SI = \left(\langle I^2\rangle - \langle I\rangle^2\right) \Big/ \langle I\rangle^2 \tag{7}$$

where $< >$ is the statistical average; I denotes the detected received light intensity, in cd.

On this technology to carry out communication distance of 12 km communication rate of 2.5 Gbps air-air laser communication experiments, test results are shown in Fig. 6. When uncontrolled, atmospheric turbulence causes fading of the received current signal, which exhibits a logarithmic distribution with a measured SI of $\sigma_I^2 = 0.2651$, and a communication BER of 2.06E-5. After the APD gain automatic control, the received current signal is more stable and shows a normal distribution, and the measured SI is $\sigma_I^2 = 0.0437$, and a communication BER of 1.35E-7.

After several measurements, the gain automatic control technique can effectively stabilize the APD output electrical signal and reduce the communication BER by more than two orders of magnitude in the medium-weak turbulence with scintillation variance of 0.01∼0.3 and 2.5 Gbps communication rate, which effectively mitigates the impact of turbulent scintillation effect on the laser communication system.

V. Channel Characteristics Test

Since the tethered airship works at an altitude of 200 m-2 km, it belongs to the near-surface atmospheric channel. Vulnerable to surface temperature changes, resulting in increased turbulence

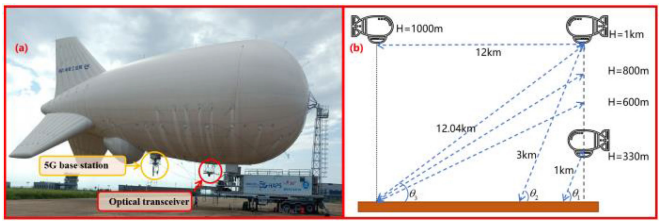

Fig. 7. (a) Blimp-borne laser communication system and 5G base station. (b) Schematic diagram of slant-range link and horizontal link test.

intensity as the atmospheric refractive index undulates. Therefore, for the special characteristics of the working channel of the airship platform, the near-ground atmospheric turbulence channel characteristics test is carried out. Since the communication system uses coarse and fine composite axis tracking system. The fine tracking bandwidth is greater than 100 Hz and the tracking accuracy is 10μrad, which can effectively suppress the blimp platform vibration (lower frequency less than 0.1 Hz), therefore, it can be considered that the platform vibration has no effect on the turbulence measurement results.

An important parameter for measuring the refractive index fluctuations in atmospheric turbulence is the refractive index structure constant C_N^2 proposed by Kolmogorov. In the horizontal link, a conversion equation exists between the refractive index structure constant and the SI.

$$\sigma_l^2 = 1.23 C_N^2 k^{7/6} L_p^{11/6} \tag{8}$$

where $k = 2\pi/\lambda$ is the wave vector, and λ is the laser carrier wavelength. L_p is the link distance in m.

The conversion relationship between the refractive index structure constant and the SI in the inclined link is expressed in the form of the integral of the atmospheric refractive index structure constant over height as follows [18].

$$\sigma_I^2 = 1.55 \overline{\xi}_k^{11/6} \int_0^1 t^{5/6} \left[C_N^2(t) / C_{N0}^2 \right] dt \tag{9}$$

where the parameter $\overline{\xi}$ is expressed in terms of the structural constant C_{N0}^2 at the reference level.

$$\overline{\xi}_k = 1.23 k^{7/11} \left(C_{N0}^2 \right)^{6/11} H / \cos\phi \tag{10}$$

where ϕ is the zenith measurement angle, k is the wave vector, and H is the vertical height. Therefore, the SI is obtained based on the real-time measurement method of channel turbulence characteristics, and the atmospheric refractive index structure constant can be calculated by Equation (8)–(10).

Based on the above theory, atmospheric turbulence SI measurements of air-air, air-ground (downlink), and ground-air (uplink) were carried out at link distances L = 1 km, 3 km, and 12 km, and the experimental link schematic is shown in Fig. 7. The measurement results are shown in Table II.

Through experiments we verified the influence of parameters such as communication link distance, airship platform height and link asymmetry on the laser communication channel. The experimental results show that the scintillation index of atmospheric turbulence increases with the increase of the link communication distance, where the maximum SI index is 0.3952 (uplink) at the communication distance of 12.01 km. With the same link distance, the SI decreases with the increasing height of the blimp platform. In the experiment, the maximum height of the blimp platform is 1km due to weather conditions, and the flicker index is 0.3657 (uplink).

TABLE II
TURBULENCE SI TEST RESULTS FOR INCLINED LINK AND THE HORIZONTAL LINK

No.	Link distance	Blimp altitude	Link	SI
1	1km	0.3km	Air-ground	0.0605
2			Ground-air	0.1105
3	3km	1km	Air-ground	0.0926
4			Ground-air	0.1597
5	12.04km	1km	Air-ground	0.2759
6			Ground-air	0.3657
7	12km		Air-air	0.2651
8	12.02km	0.8km	Air-ground	0.2918
9			Ground-air	0.3841
10	12.01km	0.6km	Air-ground	0.3097
11			Ground-air	0.3952

At the same time, we have verified for the first time the asymmetric properties of the slant-range link channel, due to the atmospheric refractive index structure constant as a function of height. The different order of the beam passing through the major/minor refractive index under the slant-range link leads to the difference in the flicker index of the communication link, reflecting the asymmetry of the channel. Under the same conditions of link distance and blimp platform height, we measured the scintillation indices of ground-air (uplink) and air-ground (downlink) by the full-duplex characteristics of the laser communication system. It is clear from many measurements that, the downlink SI is better than the uplink SI. In summary, none of the above scintillation indices reached the turbulence saturation effect, and the communication conditions were satisfied with good quality communication effects. The results of the above experiments provide a reference for the development of future communication systems in atmospheric channels.

VI. CONCLUSION

Space mobile base stations are considered to the best way to solve the problem of building wireless communication links in areas such as islands and remote mountain villages, and the blimp-borne laser communication system is an important part of information interaction between space dynamic base stations. Therefore, we design a blimp-borne laser communication system for 5G networks, using a laser communication link to transmit data from the 5G core network. In a medium-weak turbulent channel with a communication distance of 12 km, the blimp-borne laser communication system achieved technical specifications such as tracking accuracy better than 15μrad, communication rate of 2.5 Gbps, and BER of 1E-7 orders of magnitude. Based on the above experimental results, a 5G network transmission test was conducted. Under the air-air laser communication link, the average 5G physical layer data rate of 619.46 frames/second, the average 5G media access control data transmission rate of 554.74 frames/second, the 5G service packet full scheduling operation of 1400 times/second, and the 5G mobile terminal download speed greater than 1.2 Gbps were achieved. And for the special characteristics of the channel

where the blimp platform is located, the turbulence real-time measurement method based on the light intensity scintillation principle is proposed, and the real-time turbulence characteristics measurement of the blimp inclined range link and horizontal link is carried out. This experiment lays the theoretical foundation for the application of space laser communication in 5G networks and provides practical experience for the development of space base stations.

REFERENCES

[1] C. Abou-Rjeily, G. Kaddoum, and G. K. Karagiannidis, "Ground-to-air FSO communications: When high data rate communication meets efficient energy harvesting with simple designs," *Opt. Exp.*, vol. 27, no. 23, pp. 34080–34093, 2019.

[2] X. L. Li, W. Feng, J. Wang, Y. Chen, N. Ge, and C. -X. Wang, "Enabling 5G on the ocean: A hybrid satellite-uav-terrestrial network solution," *IEEE Wireless Commun.*, vol. 27, no. 6, pp. 116–121, Dec. 2020.

[3] W. Wang, Z. F. Bai, X. P. Xie, H. P. Mei, and W. Zhao, "Field experiment and analysis for free-space laser transmission characteristic in turbulent path based on MWIR and NIR," *Modern Phys. Lett. B*, vol. 34, no. 14, 2020, Art. no. 2050148.

[4] H. T. Zheng *et al.*, "Experimental demonstration of 9.6 Gbit/s polar coded infrared light communication system," *IEEE Photon. Technol. Lett.*, vol. 32, no. 24, pp. 1539–1542, Dec. 2020.

[5] J. Osborn, M. J. Townson, O. J. D. Farley, A. Reeves, and R. M. Calvo, "Adaptive optics pre-compensated laser uplink to LEO and GEO," *Opt. Exp.*, vol. 29, no. 4, pp. 6113–6132, 2021.

[6] Y. M. Li, C. Gao, M. S. Leeson, and X. F. Li, "Asymptotic analysis of V-BLAST MIMO for coherent optical wireless communications in gamma-gamma turbulence," *Opt. Exp.*, vol. 26, no. 21, pp. 27931–27944, 2018.

[7] B. Moision, B. Erkmen, E. Keyes, T. Belt, and V. William, "Demonstration of free-space optical communication for long-range data links between balloons on project loon," *Proc. SPIE*, vol. 10096, no. 14, 2017, Art. no. 100960Z.

[8] S. Y. Yu, F. Wu, Q. Wang, L. Y. Tan, and J. Ma, "Theoretical analysis and experimental study of constraint boundary conditions for acquiring the beacon in satellite–ground laser communications," *Opt. Commun.*, vol. 402, no. 1, pp. 585–592, 2017.

[9] L. Li *et al.*, "Mitigation for turbulence effects in a 40-Gbit/s orbital-angular-momentum-multiplexed free-space optical link between a ground station and a retro-reflecting UAV using MIMO equalization," *Opt. Lett.*, vol. 44, no. 21, pp. 5181–5184, 2019.

[10] X. N. Yu *et al.*, "Atmospheric turbulence suppression algorithm based on APD adaptive gain control for FSO links of 5G floating base stations," *IEEE Photon. J.*, vol. 12, no. 4, Aug. 2020, Art. no. 7904011.

[11] I. B. Djordjevic, "Adaptive modulation and coding for free-space optical channels," *IEEE/OSA J. Opt. Commun. Netw.*, vol. 2, no. 5, pp. 221–229, May 2010.

[12] F. P. Guiomar *et al.*, "Adaptive probabilistic shaped modulation for high-capacity free-space optical links," *J. Lightw. Technol.*, vol. 38, no. 23, pp. 1–13, 2020.

[13] Y. Lei, X. M. Li, and L. Z. Zhang, "Experimental study on PAT system for long-distance laser communications between fixed-wing aircrafts," *Photonic Sensors*, vol. 9, no. 2, pp. 170–178, 2019.

[14] R. X. Wu, X. Zhao, Y. Q. Liu, and Y. S. Song, "Initial pointing technology of line of sight and its experimental testing in dynamic laser communication system," *IEEE Photon. J.*, vol. 11, no. 2, Apr. 2019, Art. no. 7903008.

[15] J. Ma, G. Y. Lu, S. Y. Yu, and L. Y. Tan, "Acquisition performance analysis for intersatellite optical communications with vibration influence project supported by the program of excellent team in Harbin Institute of Technology," *Chin. Phys. B*, vol. 29, no. 1, 2020, Art. no. 014205.

[16] Y. P. Xie, T. Lei, C. W. Yang, L. P. Du, and X. C. Yuan, "Beam wander relieved optical switch using bessel beams in turbulent atmosphere," *Chin. Opt. Lett.*, vol. 17, no. 9, pp. 14–18, 2019.

[17] C. Liu, Y. Yao, Y. X. Sun, and X. H. Zhao, "Analysis of average capacity for free-space optical links with pointing errors over gamma-gamma turbulence channels," *Chin. Opt. Lett.*, vol. 8, no. 6, pp. 537–540, 2010.

[18] M. J. Beran and A. M. Whitman, "Scintillation index calculations using an altitude-dependent structure constant," *Appl. Opt.*, vol. 27, no. 11, pp. 2178–2182, 1988.